

*Supplement to*

**Technical Note: Comparison of radiometric techniques for estimating recent organic carbon sequestration rates in freshwater mineral soil wetlands**

Purbasha Mistry<sup>1</sup>, Irena F. Creed<sup>1,2\*</sup>, Charles G. Trick<sup>3</sup>, Eric Enanga<sup>2</sup>, David A. Lobb<sup>4</sup>

<sup>1</sup> School of Environment and Sustainability, University of Saskatchewan, 117 Science Place, Saskatoon, SK, S7N 5C8, Canada

<sup>2</sup> Department of Physical and Environmental Sciences, University of Toronto, 1265 Military Trail, Toronto, ON, M1C 1A4, Canada

<sup>3</sup> Department of Health and Society, University of Toronto, 1265 Military Trail, Toronto, ON, M1C 1A4, Canada

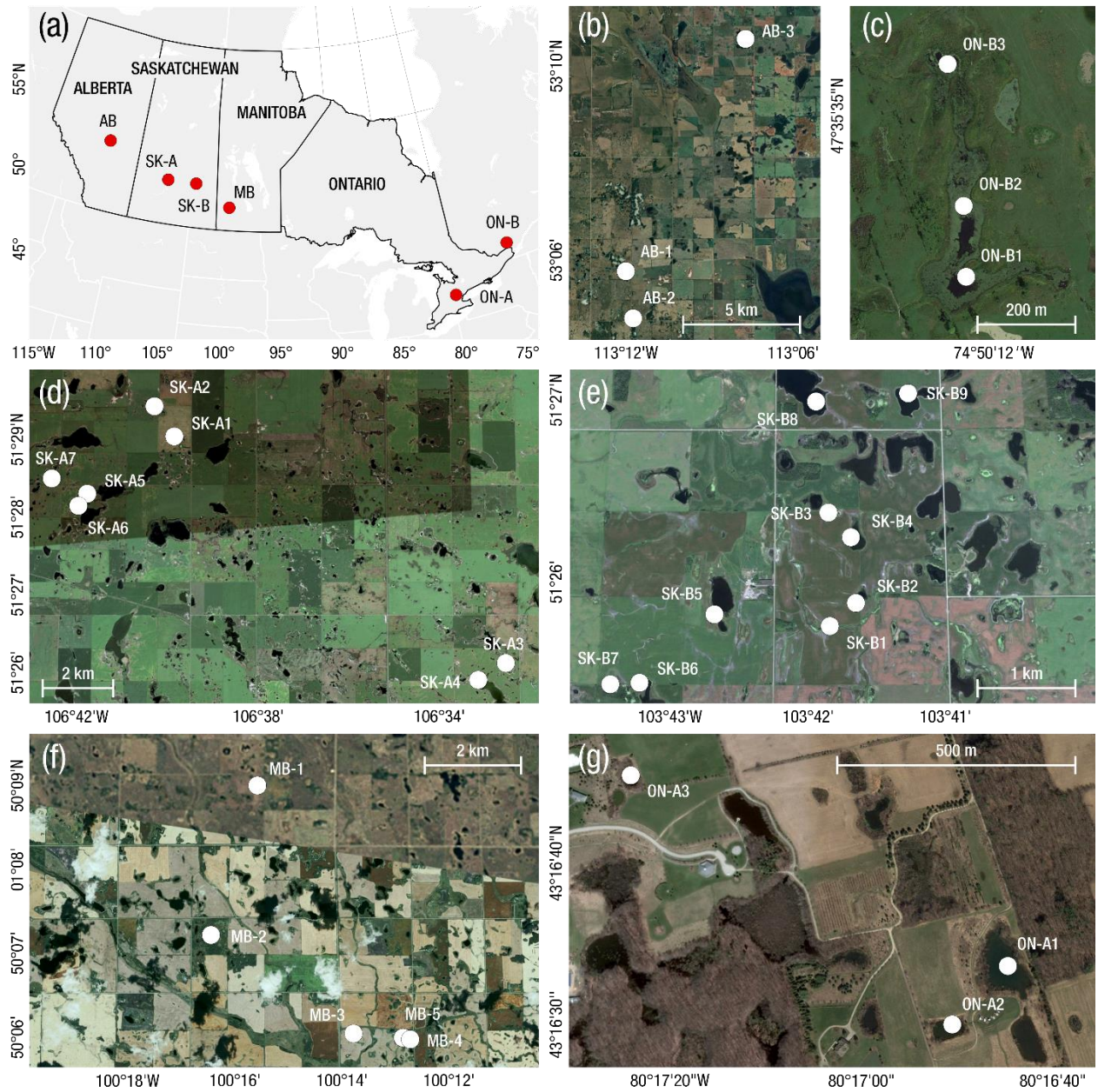
<sup>4</sup> Department of Soil Science, University of Manitoba, 13 Freedman Crescent, Winnipeg, MB, R3T 2N2, Canada

\*Correspondence to: Irena F. Creed (irena.creed@utoronto.ca)

## Table of contents

<b>Supplementary Figure 1:</b> (a) Study area situated in four provinces of Canada; (b) Alberta (AB) wetland sites; (c) Ontario (ON-B) wetland sites; (d) Saskatchewan (SK-A) wetland sites; (e) Saskatchewan (SK-B) wetland sites; (f) Manitoba (MB) wetland sites; and (g) Ontario (ON-A) wetland sites. Figures (b)-(g) are based on the sampling locations of wetlands used in this study reproduced using Google Earth Images [(b) and (c) ©2024 Airbus; (d), (e), and (g) ©2024 Maxar Technologies; (f) ©2024 Airbus and Maxar Technologies].	3
<b>Supplementary Table 1:</b> Summary of physical characteristics of wetlands.	4
<b>Supplementary Table 2:</b> Organic carbon (OC) sequestration rates and their associated classification of 44 sediment cores where both $^{137}\text{Cs}$ and $^{210}\text{Pb}$ profiles were available.	5
<b>Supplementary Figure 2:</b> Depth distributions of high-quality $^{137}\text{Cs}$ ( $\text{Bq kg}^{-1}$ ) and high-quality $^{210}\text{Pb}$ ( $\text{Bq kg}^{-1}$ ) profiles (along with the organic carbon [OC in %] concentrations and linear plot of log-transformed $^{210}\text{Pb}_{\text{ex}}$ against mass in $\text{g cm}^{-2}$ ) based on their classification. The four depth distribution plots are from sediment cores (a) AB-2 T3, (b) SK-A2 T2, (c) SK-A3 T2, and (d) SK-A3 T3.	6
<b>Supplementary Figure 3:</b> Depth distributions of high-quality $^{137}\text{Cs}$ ( $\text{Bq kg}^{-1}$ ) and high-quality $^{210}\text{Pb}$ ( $\text{Bq kg}^{-1}$ ) profiles (along with the organic carbon [OC in %] concentrations and linear plot of log-transformed $^{210}\text{Pb}_{\text{ex}}$ against mass in $\text{g cm}^{-2}$ ) based on their classification. The four depth distribution plots are from sediment cores (a) SK-A4 T2, (b) SK-A5 T1, (c) SK-A5 T3, and (d) SK-A7 T1.	7
<b>Supplementary Figure 4:</b> Depth distributions of high-quality $^{137}\text{Cs}$ ( $\text{Bq kg}^{-1}$ ) and high-quality $^{210}\text{Pb}$ ( $\text{Bq kg}^{-1}$ ) profiles (along with the organic carbon [OC in %] concentrations and linear plot of log-transformed $^{210}\text{Pb}_{\text{ex}}$ against mass in $\text{g cm}^{-2}$ ) based on their classification. The four depth distribution plots are from sediment cores (a) SK-A7 T2, (b) SK-A7 T3, (c) SK-B1 T2, and (d) SK-B1 T3.	8
<b>Supplementary Figure 5:</b> Depth distributions of high-quality $^{137}\text{Cs}$ ( $\text{Bq kg}^{-1}$ ) and high-quality $^{210}\text{Pb}$ ( $\text{Bq kg}^{-1}$ ) profiles (along with the organic carbon [OC in %] concentrations and linear plot of log-transformed $^{210}\text{Pb}_{\text{ex}}$ against mass in $\text{g cm}^{-2}$ ) based on their classification. The four depth distribution plots are from sediment cores (a) SK-B2 T2, (b) SK-B4 T1, (c) SK-B4 T2, and (d) SK-B4 T3.	9
<b>Supplementary Figure 6:</b> Depth distributions of high-quality $^{137}\text{Cs}$ ( $\text{Bq kg}^{-1}$ ) and high-quality $^{210}\text{Pb}$ ( $\text{Bq kg}^{-1}$ ) profiles (along with the organic carbon [OC in %] concentrations and linear plot of log-transformed $^{210}\text{Pb}_{\text{ex}}$ against mass in $\text{g cm}^{-2}$ ) based on their classification. The four depth distribution plots are from sediment cores (a) SK-B5 T1, (b) SK-B5 T3, (c) SK-B9 T2, and (d) SK-B9 T3.	10
<b>Supplementary Figure 7:</b> Depth distributions of high-quality $^{137}\text{Cs}$ ( $\text{Bq kg}^{-1}$ ) and high-quality $^{210}\text{Pb}$ ( $\text{Bq kg}^{-1}$ ) profiles (along with the organic carbon [OC in %] concentrations and linear plot of log-transformed $^{210}\text{Pb}_{\text{ex}}$ against mass in $\text{g cm}^{-2}$ ) based on their classification. The four depth distribution plots are from sediment cores (a) MB-1 T1, (b) MB-1 T2, (c) MB-1 T3, and (d) MB-2 T1.	11
<b>Supplementary Figure 8:</b> Depth distributions of high-quality $^{137}\text{Cs}$ ( $\text{Bq kg}^{-1}$ ) and high-quality $^{210}\text{Pb}$ ( $\text{Bq kg}^{-1}$ ) profiles (along with the organic carbon [OC in %] concentrations and linear plot of log-transformed $^{210}\text{Pb}_{\text{ex}}$ against mass in $\text{g cm}^{-2}$ ) based on their classification. The four depth distribution plots are from sediment cores (a) MB-4 T1, (b) MB-4 T2, (c) ON-A1 T2, and (d) ON-A1 T3.	12

<b>Supplementary Figure 9:</b> Depth distributions of high-quality $^{137}\text{Cs}$ ( $\text{Bq kg}^{-1}$ ) and high-quality $^{210}\text{Pb}$ ( $\text{Bq kg}^{-1}$ ) profiles (along with the organic carbon [OC in %] concentrations and linear plot of log-transformed $^{210}\text{Pb}_{\text{ex}}$ against mass in $\text{g cm}^{-2}$ ) based on their classification. The depth distribution plot is from sediment core ON-B2 T3.	13
<b>Supplementary Figure 10:</b> Depth distributions of high-quality $^{137}\text{Cs}$ ( $\text{Bq kg}^{-1}$ ) and low-quality $^{210}\text{Pb}$ ( $\text{Bq kg}^{-1}$ ) profiles (along with the organic carbon [OC in %] concentrations and linear plot of log-transformed $^{210}\text{Pb}_{\text{ex}}$ against mass in $\text{g cm}^{-2}$ ) based on their classification. The four depth distribution plots are from sediment cores (a) SK-B2 T3, (b) MB-3 T2, (c) MB-5 T1, and (d) MB-5 T3.	14
<b>Supplementary Figure 11:</b> Depth distributions of high-quality $^{137}\text{Cs}$ ( $\text{Bq kg}^{-1}$ ) and low-quality $^{210}\text{Pb}$ ( $\text{Bq kg}^{-1}$ ) profiles (along with the organic carbon [OC in %] concentrations and linear plot of log-transformed $^{210}\text{Pb}_{\text{ex}}$ against mass in $\text{g cm}^{-2}$ ) based on their classification. The depth distribution plot is from sediment core ON-B1 T3.	15
<b>Supplementary Figure 12:</b> Depth distributions of low-quality $^{137}\text{Cs}$ ( $\text{Bq kg}^{-1}$ ) and high-quality $^{210}\text{Pb}$ ( $\text{Bq kg}^{-1}$ ) profiles (along with the organic carbon [OC in %] concentrations and linear plot of log-transformed $^{210}\text{Pb}_{\text{ex}}$ against mass in $\text{g cm}^{-2}$ ) based on their classification. The four depth distribution plots are from sediment cores (a) ON-A2 T2, (b) ON-A2 T3, (c) ON-A2 T3, and (d) ON-B1 T1.	16
<b>Supplementary Figure 13:</b> Depth distributions of low-quality $^{137}\text{Cs}$ ( $\text{Bq kg}^{-1}$ ) and high-quality $^{210}\text{Pb}$ ( $\text{Bq kg}^{-1}$ ) profiles (along with the organic carbon [OC in %] concentrations and linear plot of log-transformed $^{210}\text{Pb}_{\text{ex}}$ against mass in $\text{g cm}^{-2}$ ) based on their classification. The two depth distribution plots are from sediment cores (a) ON-B1 T2 and (b) ON-B3 T1.	17



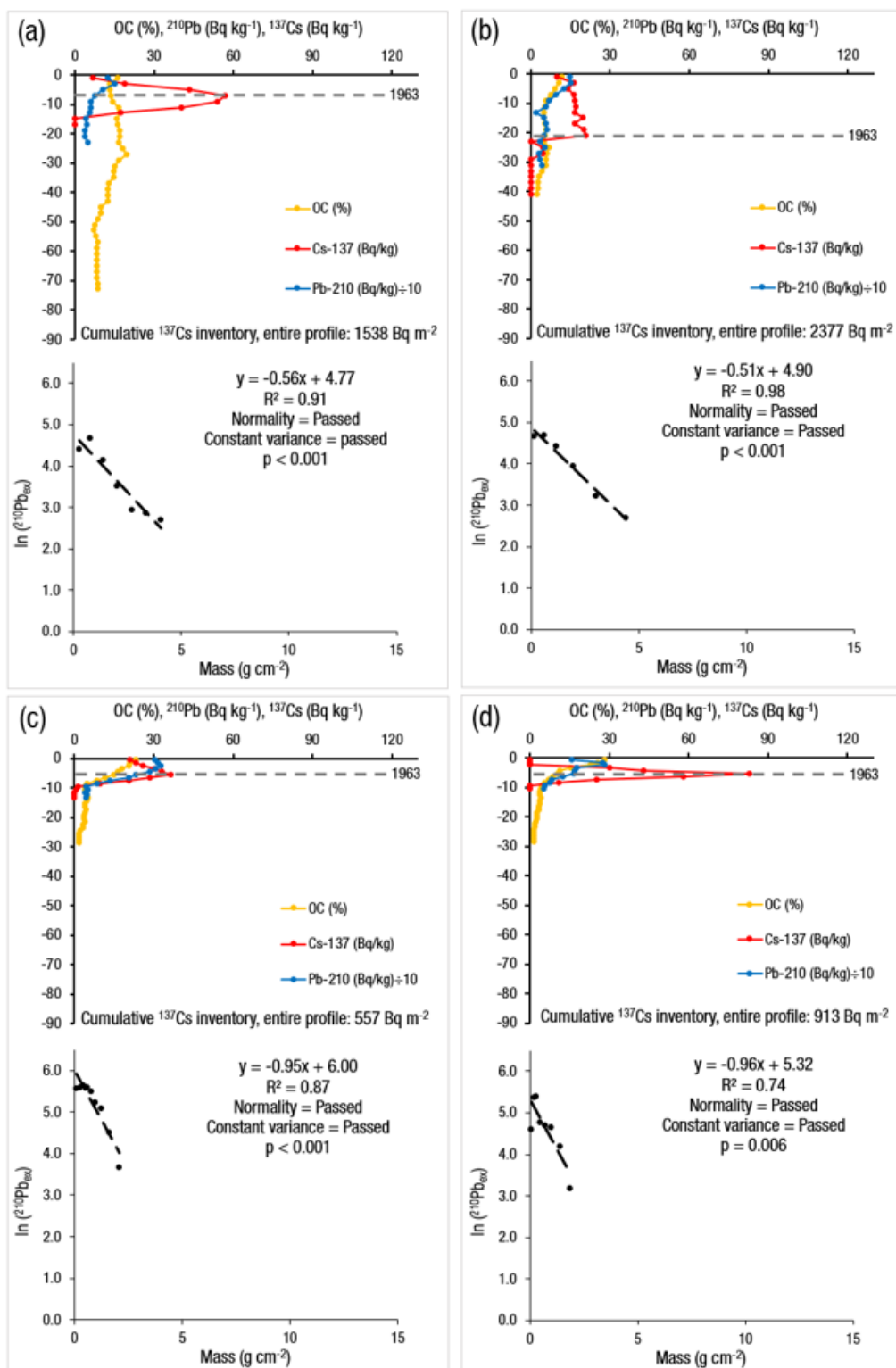
**Supplementary Figure 1:** (a) Study area situated in four provinces of Canada; (b) Alberta (AB) wetland sites; (c) Ontario (ON-B) wetland sites; (d) Saskatchewan (SK-A) wetland sites; (e) Saskatchewan (SK-B) wetland sites; (f) Manitoba (MB) wetland sites; and (g) Ontario (ON-A) wetland sites. Figures (b)-(g) are based on the sampling locations of wetlands used in this study reproduced using Google Earth Images [(b) and (c) ©2024 Airbus; (d), (e), and (g) ©2024 Maxar Technologies; (f) ©2024 Airbus and Maxar Technologies].

**Supplementary Table 1:** Summary of physical characteristics of wetlands.

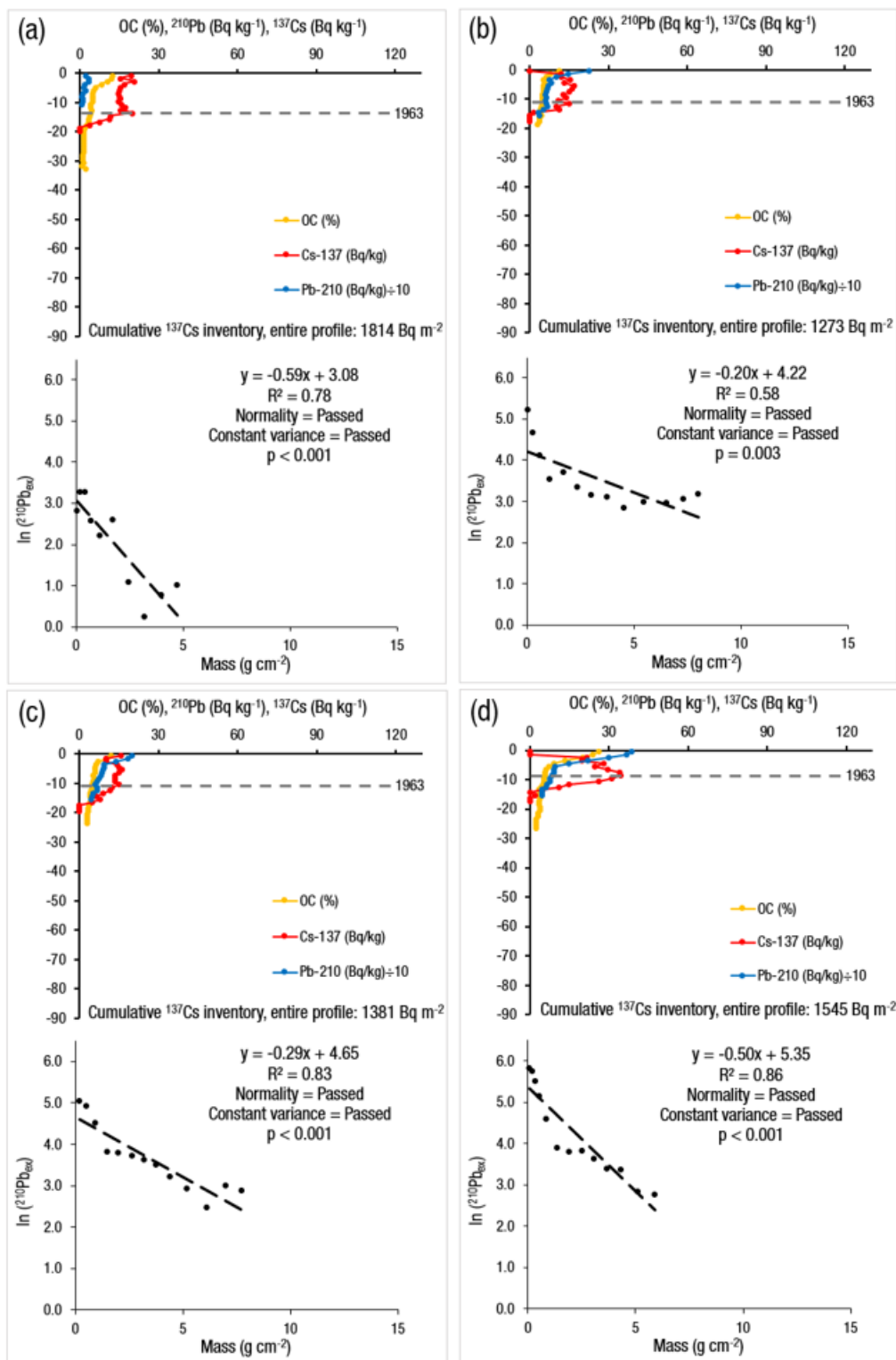
<b>Category</b>	<b>Alberta</b>	<b>Saskatchewan</b>		<b>Manitoba</b>	<b>Ontario</b>	
Province id	AB	SK-A	SK-B	MB	ON-A	ON-B
Number of wetlands	3	7	9	5	3	3
Latitude and longitude	52°- 53° and 111°- 113°	51° and 106°	51° and 103°	50° and 100°	43.3° and 80.3°	45.6° and 74.8°
Sampling year	2016	2019	2019	2019	2018	2019
Mean temperature of the growing season (°C)	11	12.1	11.7	12.4	14.3	13.8
Mean total annual precipitation of the water year (mm)	439	360	458	464	892	997
Hardiness zone	3b	3b	3a	3a	5b	5a
Proportion of hardiness	1	1	1	0.7	0.7	1
Soil great group	Black Chernozem	Dark Brown Chernozem	Black Chernozem	Black Chernozem	Grey Brown Luvisol	Humic Gleysol
Soil texture	Fine	Medium	Medium	Fine	Coarse	Fine
Local surface form	Hummocky and undulating	Hummock, undulating, and ridged	Hummocky	Hummocky	Hummocky	Level
Regional slope (%)	0-9	0-9	4-9	4-9	10-15	0-3
Drainage class	Well drained	Well drained	Well drained	Well drained	Well drained	Poorly drained

**Supplementary Table 2:** Organic carbon (OC) sequestration rates based on  $^{137}\text{Cs}$  and  $^{210}\text{Pb}$  dating and their associated classification of 44 sediment cores (where both  $^{137}\text{Cs}$  and  $^{210}\text{Pb}$  profiles were available).

Wetland id	Classification of $^{137}\text{Cs}$	Classification of $^{210}\text{Pb}$	OC sequestration rate since 1954, $^{137}\text{Cs}$ ( $\text{Mg ha}^{-1} \text{yr}^{-1}$ )	OC sequestration rate since 1963, $^{137}\text{Cs}$ ( $\text{Mg ha}^{-1} \text{yr}^{-1}$ )	OC sequestration rate since 1954, $^{210}\text{Pb}$ ( $\text{Mg ha}^{-1} \text{yr}^{-1}$ )	OC sequestration rate since 1963, $^{210}\text{Pb}$ ( $\text{Mg ha}^{-1} \text{yr}^{-1}$ )
AB-2 T3	High-quality	High-quality	1.04	0.62	0.80	0.78
SK-A1 T3	Low-quality	High-quality	0.32	0.27	0.31	0.33
SK-A2 T2	High-quality	High-quality	1.62	1.38	0.47	0.49
SK-A3 T1	High-quality	High-quality	0.64	0.37	0.37	0.40
SK-A3 T2	High-quality	High-quality	0.56	0.37	0.45	0.50
SK-A3 T3	High-quality	High-quality	0.47	0.34	0.40	0.43
SK-A4 T2	High-quality	High-quality	0.93	0.84	0.35	0.36
SK-A5 T1	High-quality	High-quality	0.84	0.68	0.80	0.83
SK-A5 T3	High-quality	High-quality	1.00	0.75	0.68	0.70
SK-A6 T1	Low-quality	Low-quality	0.11	0.05	0.69	0.73
SK-A7 T1	High-quality	High-quality	0.86	0.55	0.53	0.56
SK-A7 T2	High-quality	High-quality	0.57	0.30	0.41	0.43
SK-A7 T3	High-quality	High-quality	0.69	0.60	0.54	0.56
SK-B1 T2	High-quality	High-quality	1.01	0.83	0.81	0.81
SK-B1 T3	High-quality	High-quality	0.88	0.83	0.77	0.77
SK-B2 T2	High-quality	High-quality	0.58	0.34	0.34	0.34
SK-B2 T3	High-quality	Low-quality	0.44	0.37	0.60	0.63
SK-B4 T1	High-quality	High-quality	1.70	1.57	1.41	1.36
SK-B4 T2	High-quality	High-quality	1.31	1.14	0.69	0.71
SK-B4 T3	High-quality	High-quality	1.04	1.03	0.95	0.95
SK-B5 T1	High-quality	High-quality	1.25	0.65	1.04	1.04
SK-B5 T3	High-quality	High-quality	1.16	0.76	0.71	0.71
SK-B9 T2	High-quality	High-quality	0.67	0.50	0.59	0.60
SK-B9 T3	High-quality	High-quality	1.18	0.38	0.46	0.46
MB-1 T1	High-quality	High-quality	1.60	0.39	0.51	0.53
MB-1 T2	High-quality	High-quality	1.11	0.91	0.97	1.01
MB-1 T3	High-quality	High-quality	0.99	0.50	0.60	0.63
MB-2 T1	High-quality	High-quality	0.98	0.12	1.08	1.15
MB-3 T2	High-quality	Low-quality	1.16	0.55	0.50	0.52
MB-4 T1	High-quality	High-quality	0.44	0.21	0.34	0.36
MB-4 T2	High-quality	High-quality	0.65	0.45	0.43	0.46
MB-4 T3	High-quality	Low-quality	0.78	0.06	0.81	0.86
MB-5 T1	High-quality	Low-quality	1.03	0.26	0.38	0.39
MB-5 T3	High-quality	Low-quality	1.66	1.55	1.80	1.93
ON-A1 T2	High-quality	High-quality	1.22	0.48	0.74	0.74
ON-A1 T3	High-quality	High-quality	1.05	0.21	1.03	1.04
ON-A2 T1	Low-quality	High-quality	0.53	0.21	0.42	0.40
ON-A2 T2	Low-quality	High-quality	0.26	0.19	0.33	0.36
ON-A2 T3	Low-quality	High-quality	0.62	0.37	0.55	0.54
ON-B1 T1	Low-quality	High-quality	0.60	0.10	0.80	0.87
ON-B1 T2	Low-quality	High-quality	1.14	0.05	0.79	0.74
ON-B1 T3	High-quality	Low-quality	2.31	1.58	0.73	0.75
ON-B2 T3	High-quality	High-quality	2.60	0.76	0.76	0.76
ON-B3 T1	Low-quality	High-quality	1.15	0.12	0.23	0.23

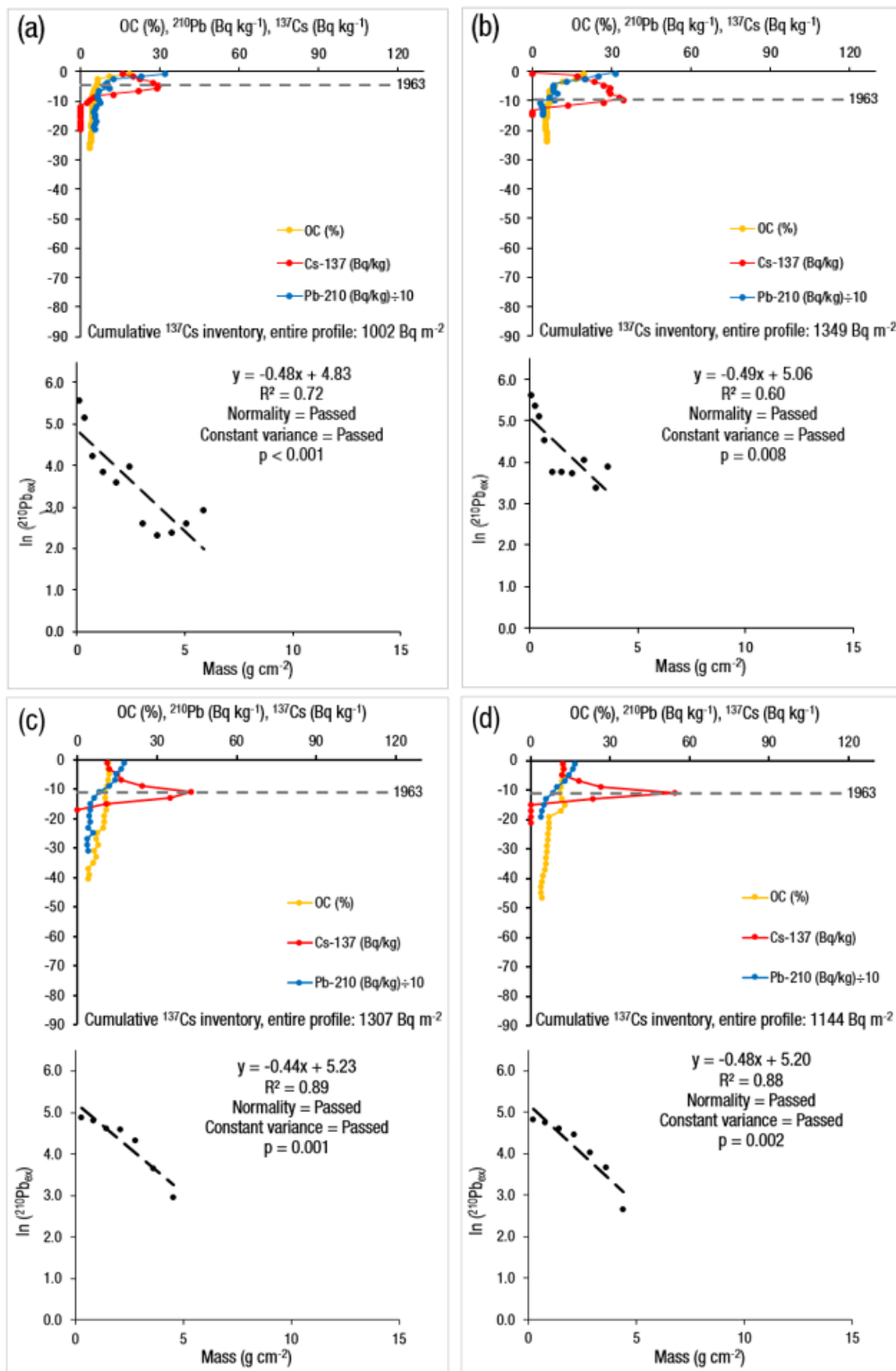


**Supplementary Figure 2:** Depth distributions of high-quality  $^{137}\text{Cs}$  (Bq kg $^{-1}$ ) and high-quality  $^{210}\text{Pb}$  (Bq kg $^{-1}$ ) profiles (along with the organic carbon [OC in %] concentrations and linear plot of log-transformed  $^{210}\text{Pb}_{\text{ex}}$  against mass in g cm $^{-2}$ ) based on their classification. The four depth distribution plots are from sediment cores (a) AB-2 T3, (b) SK-A2 T2, (c) SK-A3 T2, and (d) SK-A3 T3.

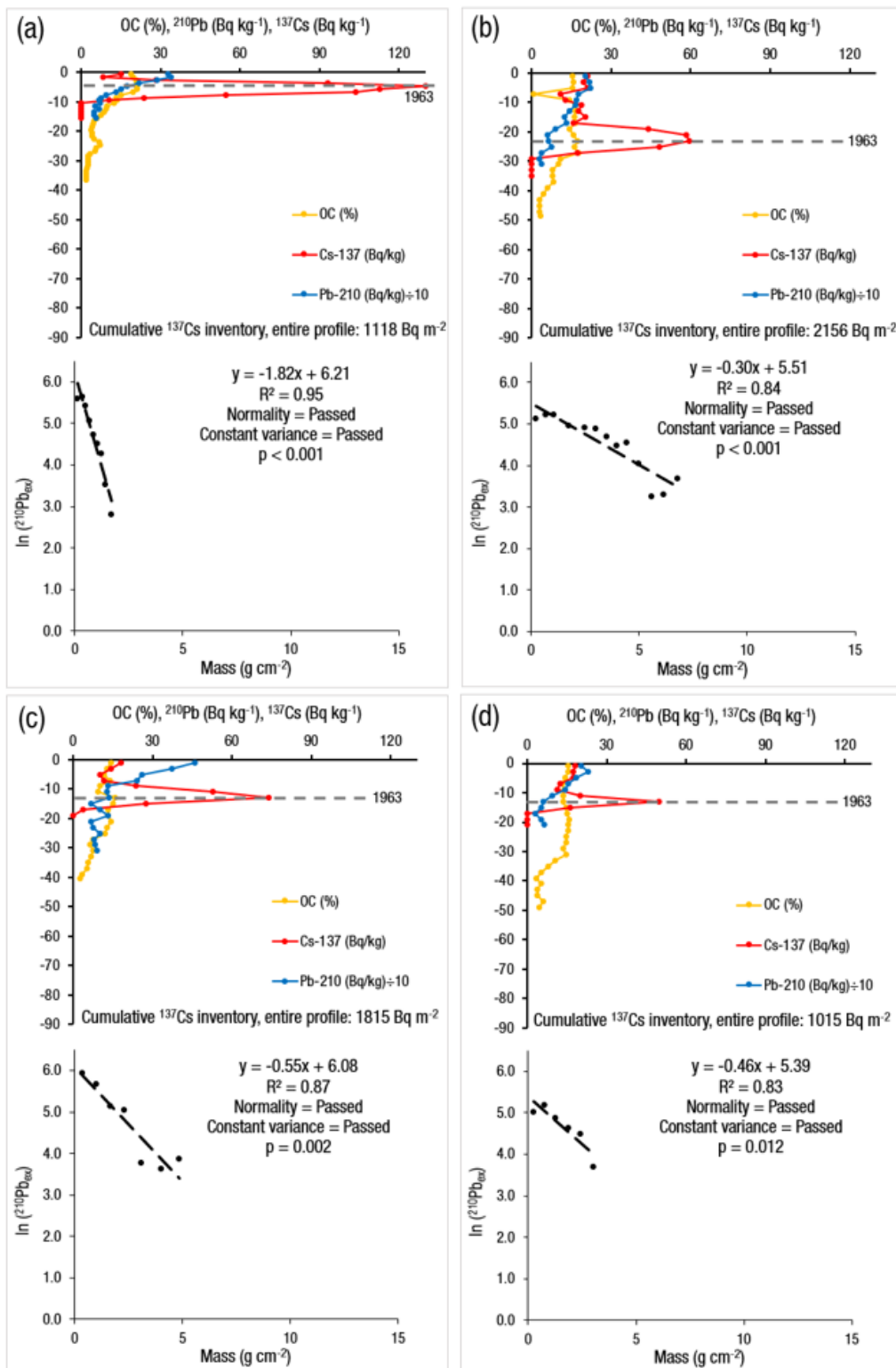


**Supplementary Figure 3:** Depth distributions of high-quality  $^{137}\text{Cs}$  ( $\text{Bq kg}^{-1}$ ) and high-quality  $^{210}\text{Pb}$  ( $\text{Bq kg}^{-1}$ ) profiles (along with the organic carbon [OC in %] concentrations and linear plot of log-transformed  $^{210}\text{Pb}_{\text{ex}}$  against mass in  $\text{g cm}^{-2}$ ) based on their classification. The four depth distribution plots are from sediment cores (a) SK-A4 T2, (b) SK-A5 T1, (c) SK-A5 T3, and (d) SK-A7 T1.

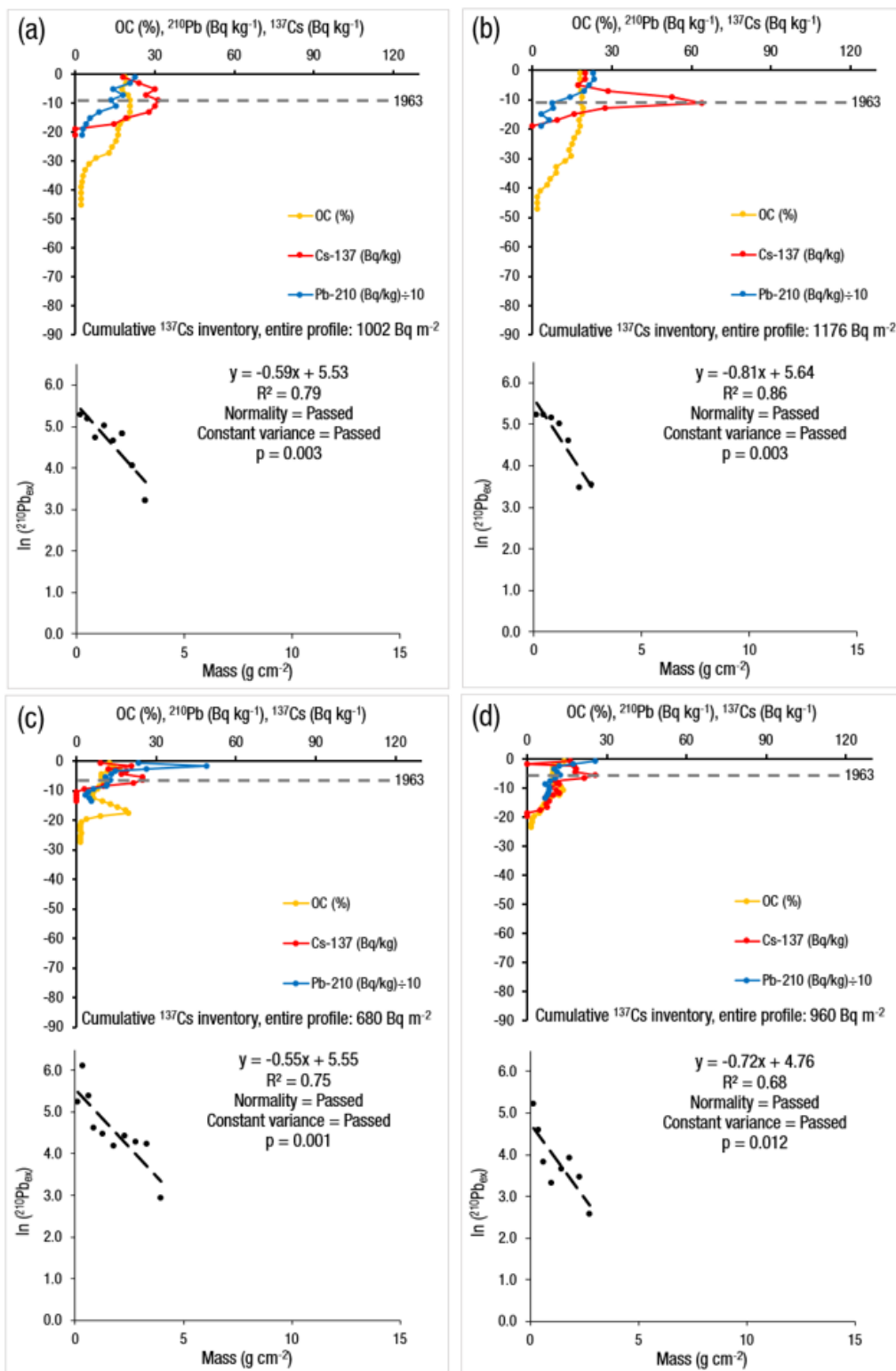




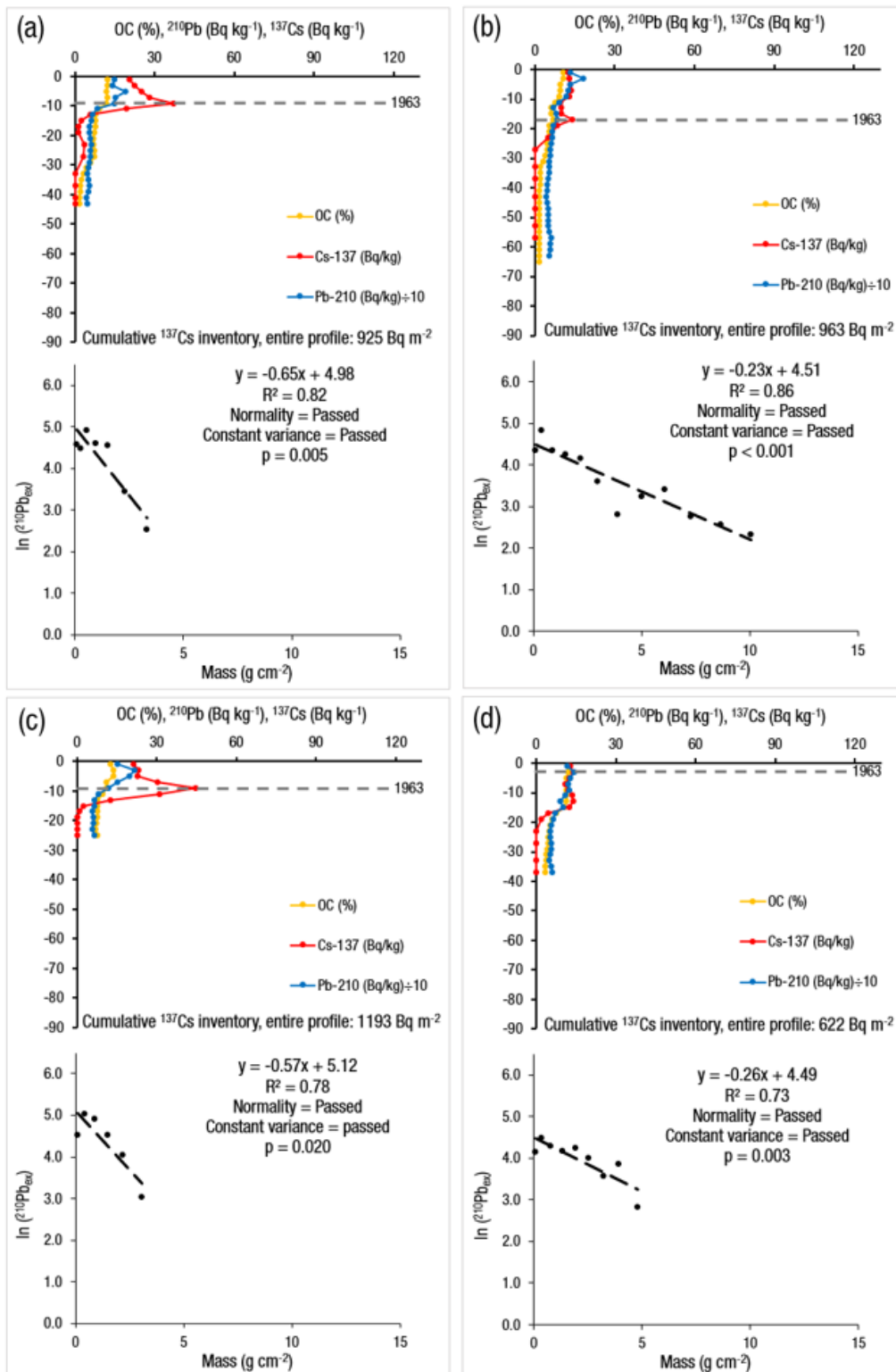
**Supplementary Figure 4:** Depth distributions of high-quality  $^{137}\text{Cs}$  (Bq kg $^{-1}$ ) and high-quality  $^{210}\text{Pb}$  (Bq kg $^{-1}$ ) profiles (along with the organic carbon [OC in %] concentrations and linear plot of log-transformed  $^{210}\text{Pb}_{\text{ex}}$  against mass in  $\text{g cm}^{-2}$ ) based on their classification. The four depth distribution plots are from sediment cores (a) SK-A7 T2, (b) SK-A7 T3, (c) SK-B1 T2, and (d) SK-B1 T3.



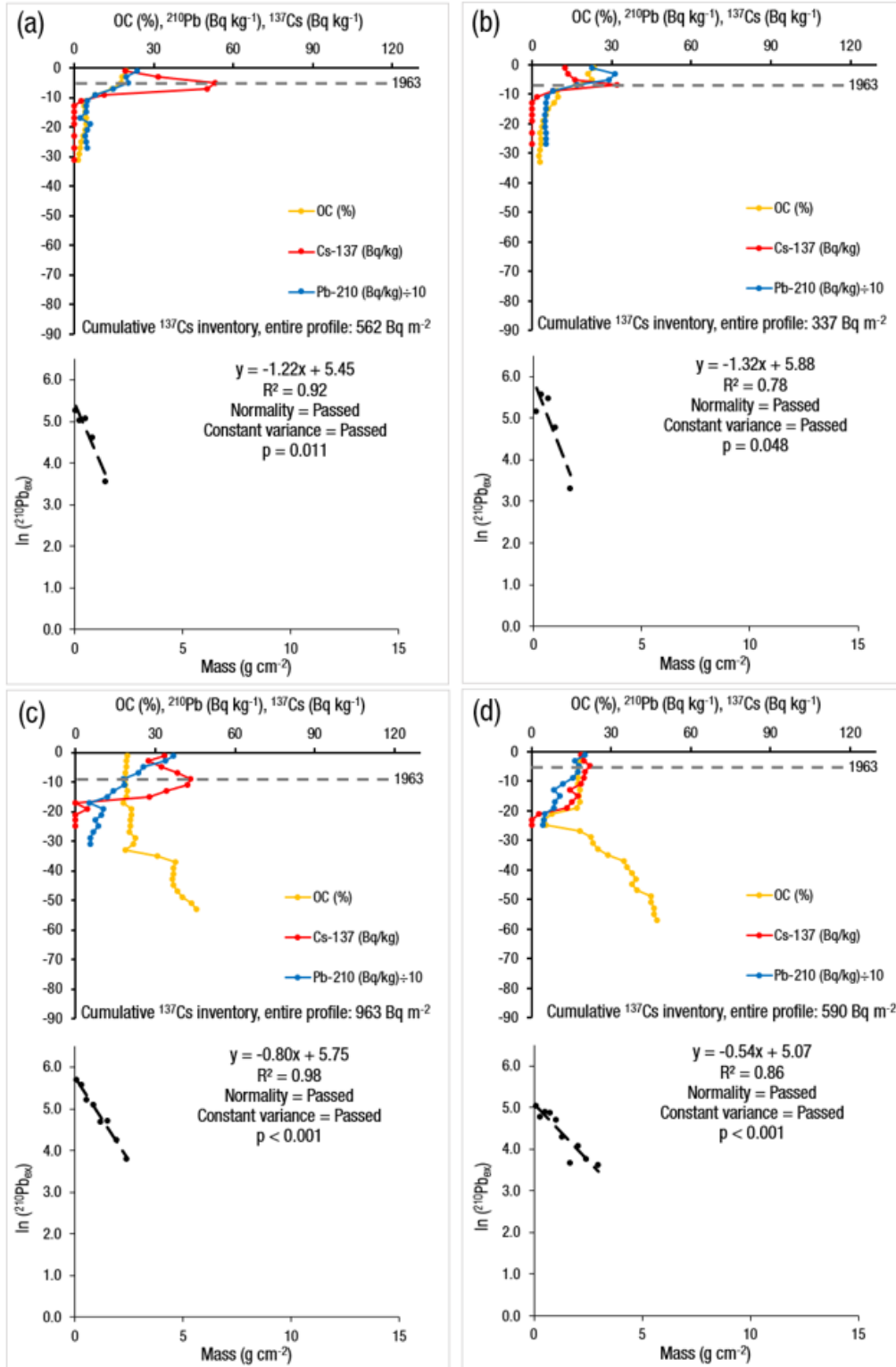
**Supplementary Figure 5:** Depth distributions of high-quality  $^{137}\text{Cs}$  ( $\text{Bq kg}^{-1}$ ) and high-quality  $^{210}\text{Pb}$  ( $\text{Bq kg}^{-1}$ ) profiles (along with the organic carbon [OC in %] concentrations and linear plot of log-transformed  $^{210}\text{Pb}_{\text{ex}}$  against mass in  $\text{g cm}^{-2}$ ) based on their classification. The four depth distribution plots are from sediment cores (a) SK-B2 T2, (b) SK-B4 T1, (c) SK-B4 T2, and (d) SK-B4 T3.



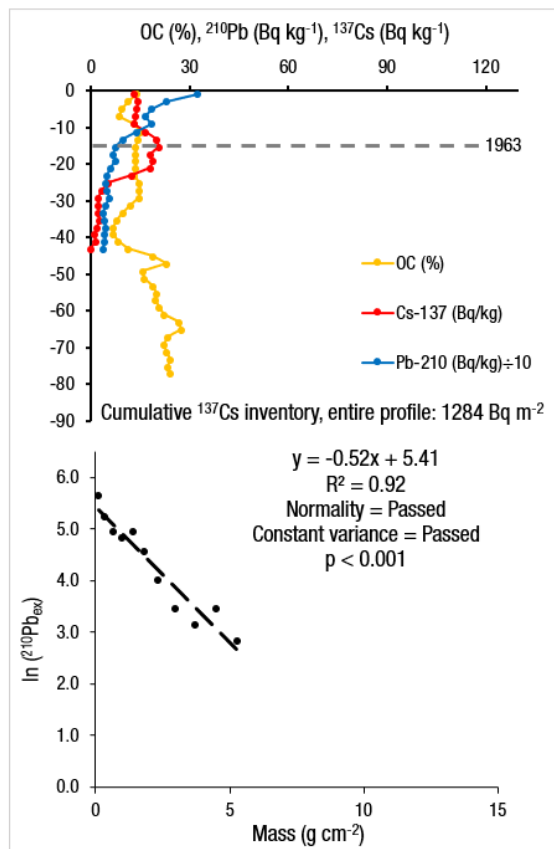
**Supplementary Figure 6:** Depth distributions of high-quality  $^{137}\text{Cs}$  ( $\text{Bq kg}^{-1}$ ) and high-quality  $^{210}\text{Pb}$  ( $\text{Bq kg}^{-1}$ ) profiles (along with the organic carbon [OC in %] concentrations and linear plot of log-transformed  $^{210}\text{Pb}_{\text{ex}}$  against mass in  $\text{g cm}^{-2}$ ) based on their classification. The four depth distribution plots are from sediment cores (a) SK-B5 T1, (b) SK-B5 T3, (c) SK-B9 T2, and (d) SK-B9 T3.



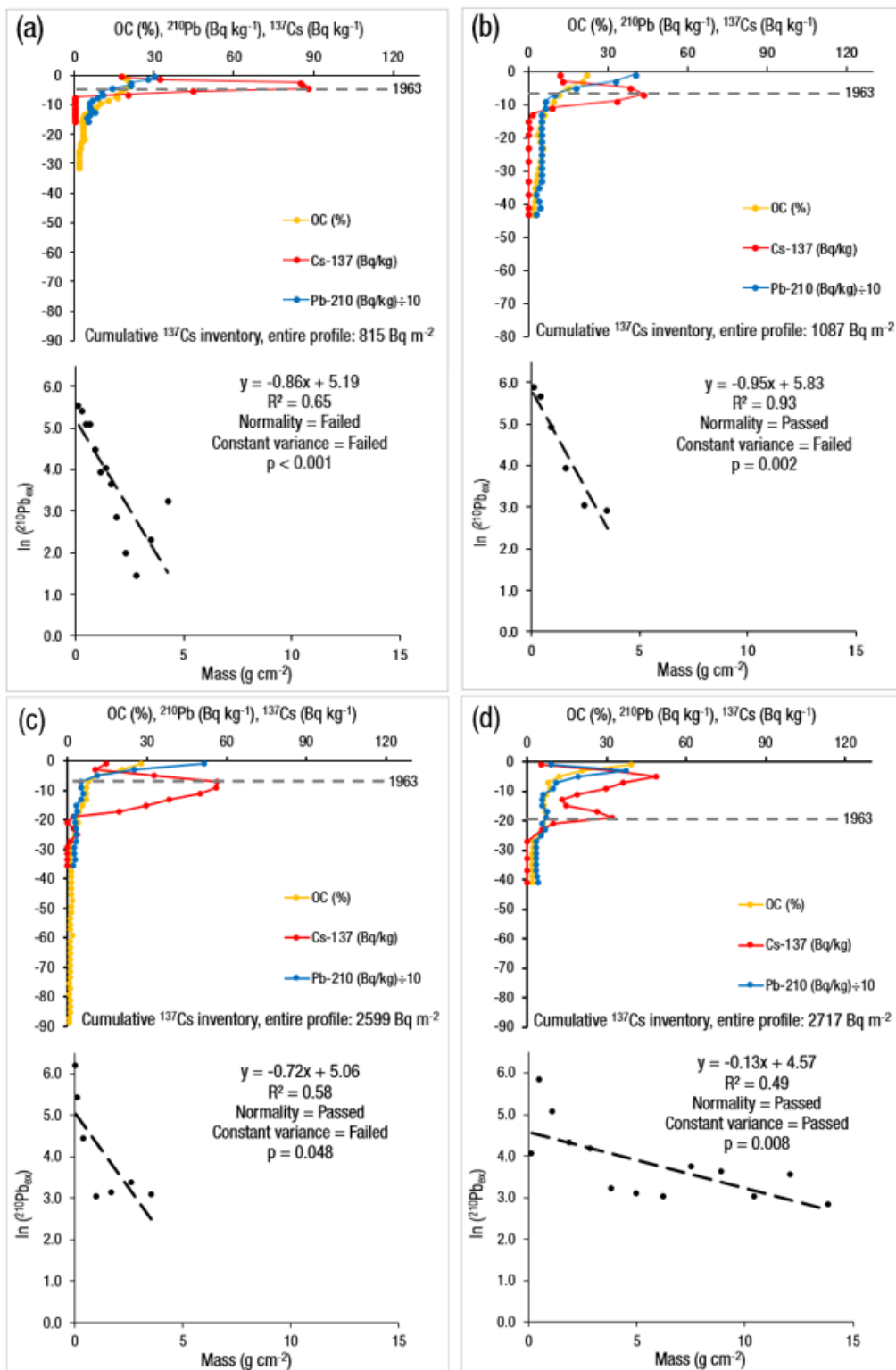
**Supplementary Figure 7:** Depth distributions of high-quality  $^{137}\text{Cs}$  (Bq kg $^{-1}$ ) and high-quality  $^{210}\text{Pb}$  (Bq kg $^{-1}$ ) profiles (along with the organic carbon [OC in %] concentrations and linear plot of log-transformed  $^{210}\text{Pb}_{\text{ex}}$  against mass in g cm $^{-2}$ ) based on their classification. The four depth distribution plots are from sediment cores (a) MB-1 T1, (b) MB-1 T2, (c) MB-1 T3, and (d) MB-2 T1.



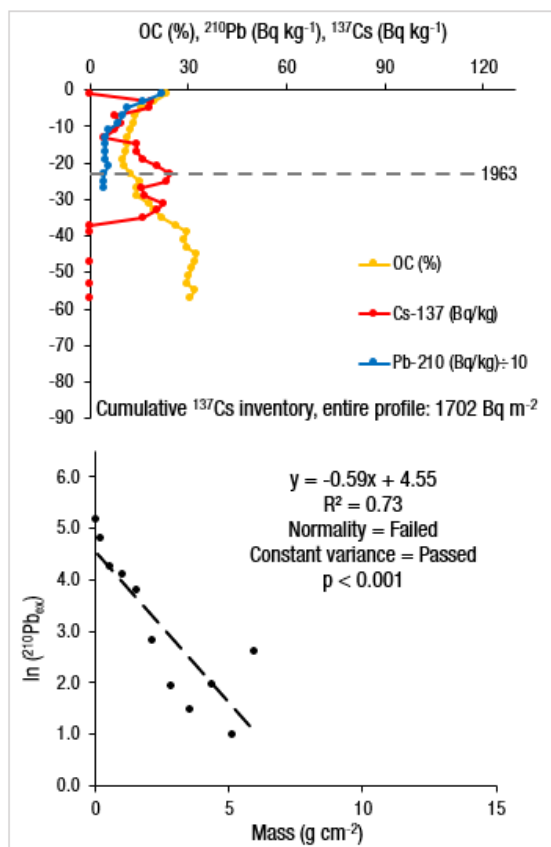
**Supplementary Figure 8:** Depth distributions of high-quality  $^{137}\text{Cs}$  ( $\text{Bq kg}^{-1}$ ) and high-quality  $^{210}\text{Pb}$  ( $\text{Bq kg}^{-1}$ ) profiles (along with the organic carbon [OC in %] concentrations and linear plot of log-transformed  $^{210}\text{Pb}_{\text{ex}}$  against mass in  $\text{g cm}^{-2}$ ) based on their classification. The four depth distribution plots are from sediment cores (a) MB-4 T1, (b) MB-4 T2, (c) ON-A1 T2, and (d) ON-A1 T3.



**Supplementary Figure 9:** Depth distributions of high-quality  $^{137}\text{Cs}$  (Bq kg $^{-1}$ ) and high-quality  $^{210}\text{Pb}$  (Bq kg $^{-1}$ ) profiles (along with the organic carbon [OC in %] concentrations and linear plot of log-transformed  $^{210}\text{Pb}_{\text{ex}}$  against mass in g cm $^{-2}$ ) based on their classification. The depth distribution plot is from sediment core ON-B2 T3.

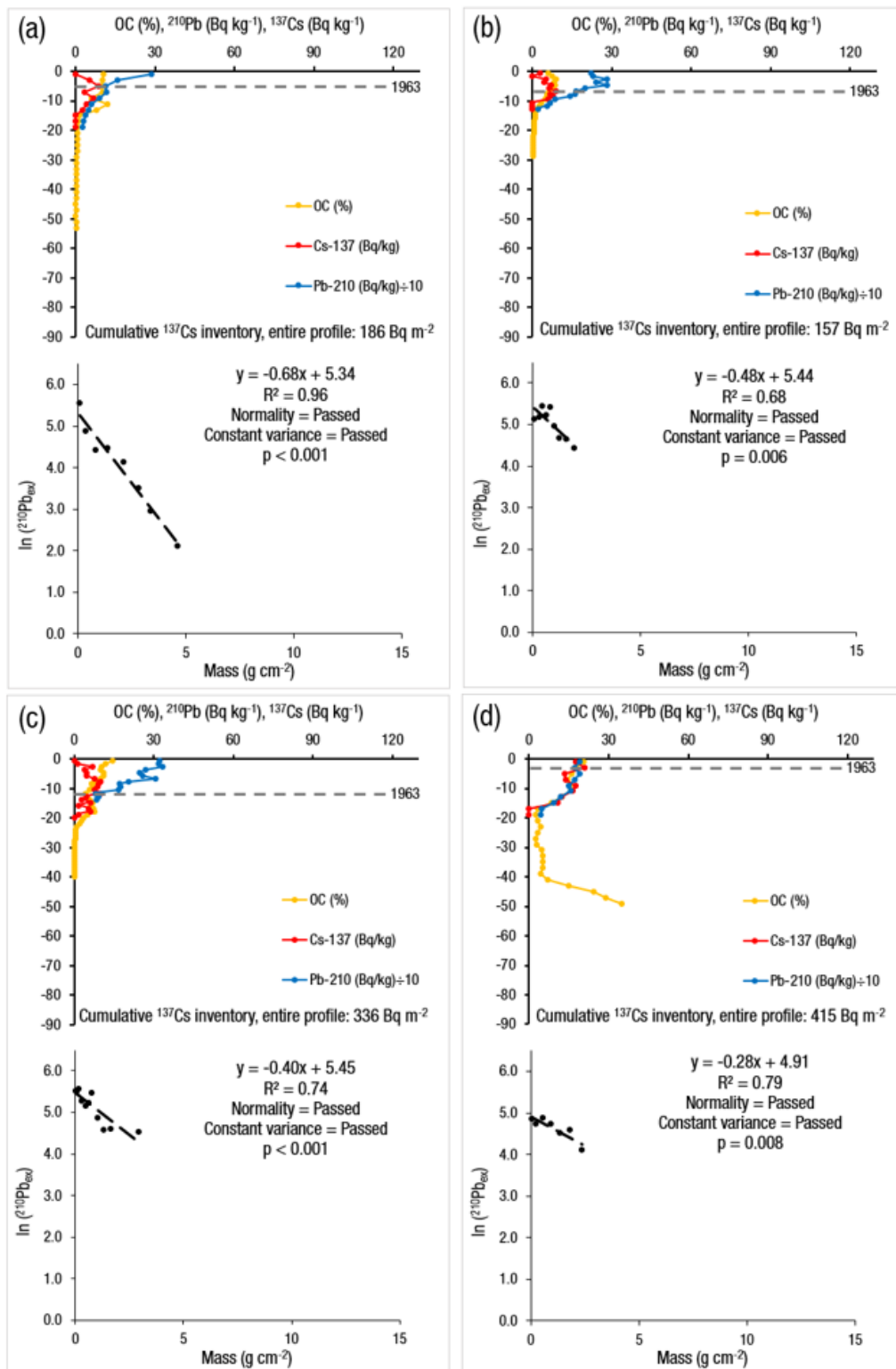


**Supplementary Figure 10:** Depth distributions of high-quality  $^{137}\text{Cs}$  ( $\text{Bq kg}^{-1}$ ) and low-quality  $^{210}\text{Pb}$  ( $\text{Bq kg}^{-1}$ ) profiles (along with the organic carbon [OC in %] concentrations and linear plot of log-transformed  $^{210}\text{Pb}_{\text{ex}}$  against mass in  $\text{g cm}^{-2}$ ) based on their classification. The four depth distribution plots are from sediment cores (a) SK-B2 T3, (b) MB-3 T2, (c) MB-5 T1, and (d) MB-5 T3.

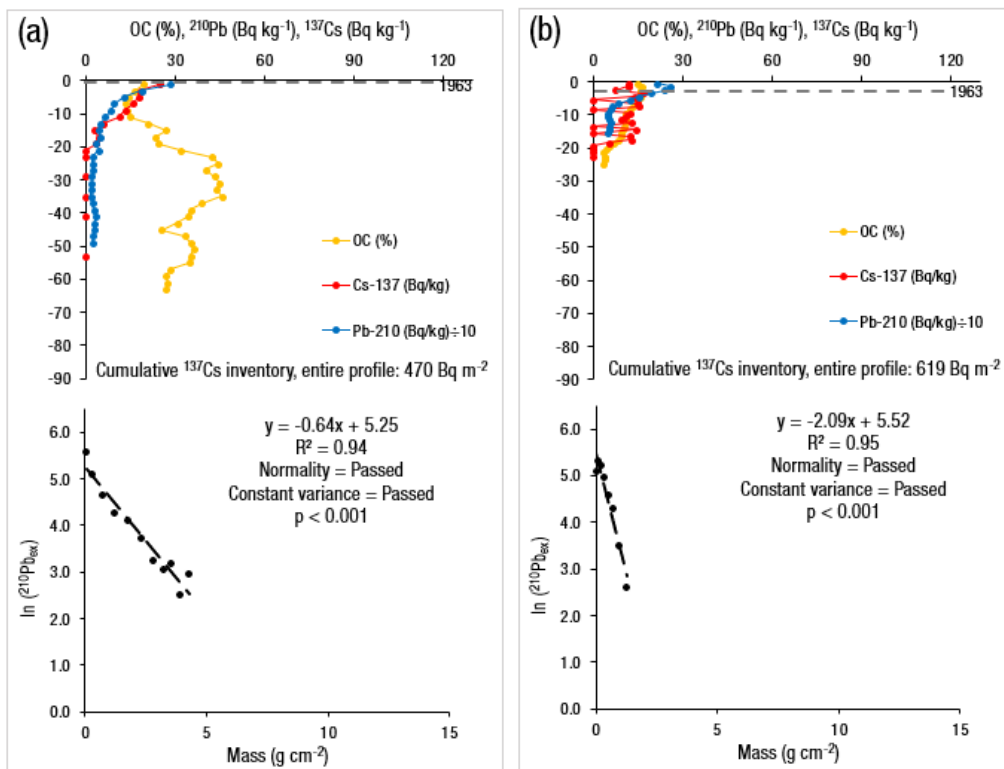


**Supplementary Figure 11:** Depth distributions of high-quality  $^{137}\text{Cs}$  (Bq kg $^{-1}$ ) and low-quality  $^{210}\text{Pb}$  (Bq kg $^{-1}$ ) profiles (along with the organic carbon [OC in %] concentrations and linear plot of log-transformed  $^{210}\text{Pb}_{\text{ex}}$  against mass in g cm $^{-2}$ ) based on their classification. The depth distribution plot is from sediment core ON-B1 T3.





**Supplementary Figure 12:** Depth distributions of low-quality  $^{137}\text{Cs}$  ( $\text{Bq kg}^{-1}$ ) and high-quality  $^{210}\text{Pb}$  ( $\text{Bq kg}^{-1}$ ) profiles (along with the organic carbon [OC in %] concentrations and linear plot of log-transformed  $^{210}\text{Pb}_{\text{ex}}$  against mass in  $\text{g cm}^{-2}$ ) based on their classification. The four depth distribution plots are from sediment cores (a) ON-A2 T2, (b) ON-A2 T3, (c) ON-A2 T3, and (d) ON-B1 T1.



**Supplementary Figure 13:** Depth distributions of low-quality  $^{137}\text{Cs}$  ( $\text{Bq kg}^{-1}$ ) and high-quality  $^{210}\text{Pb}$  ( $\text{Bq kg}^{-1}$ ) profiles (along with the organic carbon [OC in %] concentrations) and linear plot of log-transformed  $^{210}\text{Pb}_{\text{ex}}$  against mass in  $\text{g cm}^{-2}$  based on their classification. The two depth distribution plots are from sediment cores (a) ON-B1 T2 and (b) ON-B3 T1.